Measurements of the longitudinal wakefields in a multimode, dielectric wakefield accelerator driven by a train of electron bunches

J. G. Power, M. E. Conde, W. Gai, R. Konecny, and P. Schoessow
Argonne National Laboratory, 9700 South Cass Avenue, Argonne, Illinois 60439

A. D. Kanareykin
St. Petersburg Electrical Engineering University, 5 Prof. Popov Street, St. Petersburg 197376, Russia
(Received 13 July 1999; published 23 October 2000)

We report on the experimental demonstration of a novel wakefield acceleration technique where a short electron bunch excites a broadband harmonic frequency spectrum, in a cylindrical dielectric structure, to synthesize an accelerating waveform. The structure is designed to have its TM_{0n} modes nearly equally spaced so that the modes generated by a single short electron bunch constructively interfere in the neighborhood of integral multiples of the fundamental wavelength producing large acceleration gradients. Realization of a harmonic multimode structure requires more stringent design considerations than a single-mode structure, since the permittivity and loss tangent of the material should not change substantially over the bandwidth of the structure. In this experiment, a bunch train of four 5 nC electron bunches, separated by 760 ps (one net wavelength), were passed through a 60 cm long dielectric-lined cylindrical harmonic structure. Use of a train of drive bunches spaced by one wavelength reinforced the accelerating wakefield; observation of the energy loss of each bunch via a magnetic spectrometer served as a diagnostic of the wakefield. The measured energy spectrum of the four beams after passing through the waveguide was found to be in excellent agreement with the predictions of the analytic model. This result demonstrates that a dielectric can be fabricated which can synthesize the required wakefield. We also discuss potential advantages of this harmonic approach over conventional single-mode wakefield accelerators.

PACS numbers: 41.75.Lx, 41.75.Ht, 29.17.+w

I. INTRODUCTION

A recent article [1] describes a new collinear acceleration scheme in which a multimode, dielectric structure is driven by a bunch train. By multimode we mean that many of the accelerating structure's TM_{0n} ($n = 1, 2, \ldots$) modes are excited and used to synthesize an accelerating waveform of desired shape, as opposed to a conventional single-mode structure where acceleration proceeds primarily via the TM_{01} (fundamental) mode. In particular, we emphasize a class of multimode structures that possess a nearly harmonic (equally spaced in frequency) mode pattern, a state of affairs that is not generally true.

Before proceeding, a point of clarification is in order. We kept the name "multimode" chosen by the authors of Ref. [1] even though both devices described above support multiple modes. This name is somewhat appropriate since most modes in the single mode structure are not excited because most mode wavelengths are shorter than the drive bunch length. It seems clear that a better name would have been "harmonic" dielectric wakefield acceleration since this identifies a real distinction, but consistency also has its advantages.

The experiment described here was designed to investigate whether the desired longitudinal wakefield shape can be realized in the laboratory using a dielectric structure driven by a train of electron bunches. Of primary concern is whether such a device can in fact be built with currently available dielectric materials. In particular, the dielectric material used should be frequency independent in both its permittivity and its loss tangent since a variation in either one could disrupt the nearly harmonic spectrum.

To illustrate the difference between the conventional, collinear single-mode device [2] and the harmonic structure of this paper, we calculate the longitudinal wakefield in a structure of each type. Consider a single-mode structure that is a dielectric-lined, conductive, cylindrical structure (Fig. 1) of inner radius $a = 6$ mm, outer radius $b = 11.4$ mm, and dielectric constant $\varepsilon = 4.3$. For the multimode structure we use a similar device with the same a and ε, but with $b = 69.05$ mm. We assume a Gaussian longitudinal beam shape (with bunch length $\sigma_z = 2$ mm). Using the formalism of Refs. [3,4] for a drive beam on axis

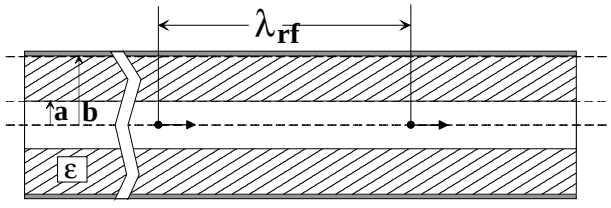

FIG. 1. The multimode waveguide driven by a bunch train (two bunches, separated by λ_{rf}, shown). The thick walled dielectric waveguide has inner radius $a = 0.5$ cm, outer radius $b = 1.44$ cm, length $L = 60$ cm, and dielectric constant $\varepsilon = 38.1$.

(i.e., $r = 0$) we have the longitudinal wake $W_z(z)$ [since $W_z(z)$ does not depend on the drive beam's transverse position, in the relativistic limit, we are justified in using this simplified approach] at distance z behind the drive electron beam,

$$W_z(z) = \int_{-\infty}^{z} dz' f(z') \left\{ \sum_{n=1}^{\infty} G_n \cos[k_n(z - z')] \right\}, \quad (1)$$

where G_n are the coefficients of the Fourier expansion, k_n are the wave numbers of the nth mode, and $f(z)$ is the axial charge distribution of the drive beam. Note that Eq. (1) holds for both the harmonic and single-mode devices, but (i) G_n and k_n are different and (ii) many more modes contribute to the wake in the harmonic device (typically $n \sim 50$) than in the single-mode device ($n \sim 1$) . In Fig. 2(a) we observe that the spatial distribution of the excited wakefield is approximately like a periodic, alternating series of delta functions separated by long regions of nearly zero field. The wakefield due to a Gaussian beam with $\sigma_z = 2$ mm is seen to decohere slightly at large z since the device is not perfectly harmonic, as will be shown in Sec. II B. Comparing the multimode wakefield with the wake due to a single-mode structure as shown Fig. 2(b), the contrast becomes apparent. The spatial distribution of the wake in the single-mode device is dominated by a single mode (TM_{01}) and therefore has a cosinelike distribution. Although the purpose of this Introduction is to point out differences between the two structures, it is interesting to note one similarity. The peak amplitude of the wakefield in both Figs. 2(a) and 2(b) is very nearly the same. This is as it must be since the total power radiated into a dielectric lined structure depends only on the inner radius "a" and dielectric constant "ε," which were chosen to be the same in this comparison [3,4].

The harmonic collinear acceleration scheme reported on in this paper may have advantages over conventional collinear wakefield devices such as improved rf breakdown properties, relaxed drive beam requirements, and reduced sensitivity to long-range parasitic wakefields. We emphasize that these are only possible advantages and, upon further analysis, may turn out not to be justified. Since the purpose of this paper is primarily to report on the measurement of the longitudinal wakefield in a harmonic structure, we will not explore all the advantages and disadvantages in enough depth to resolve the question here. In the following section we attempt to provide some motivation as to why this scheme is worthy of further study.

From the spatial distribution of the wake in Fig. 2(a), we see that the dielectric surface in a multimode structure is only exposed to a high electric field for a relatively short time. Since rf breakdown is caused by exposure to high electric fields for prolonged periods of time, we expect that these short rf pulses will allow operation at higher electric fields. By comparison, a single-mode structure, operating at the same peak electric field, has a cosinelike spatial

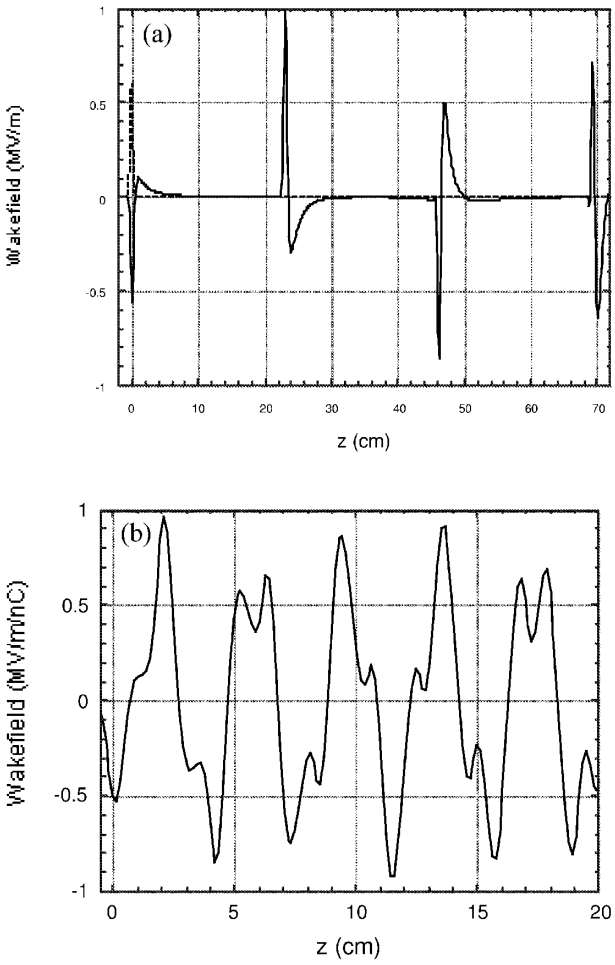

FIG. 2. (a) Longitudinal wakefield (solid line) from a single drive bunch (dashed line) located at $z = 0$ cm with bunch moving from right to left in a multimode structure. Note the cancellation of the wakefield between the peaks. (b) Longitudinal wakefield (solid line) from a single drive bunch (not shown) located at $z = 0$ cm with bunch moving from right to left in a single-mode structure. The points are the value of the wakefield at each point, and the solid line is a fit to the fundamental TM_{01} mode.

distribution, and the electric field strength is substantial over a larger portion of the device period than is necessary for acceleration.

Drive beam requirements are relaxed by dividing a single, high-charge bunch into a train of low-charge bunches with equal total charge. Since the peak wakefield is proportional to the charge, we can divide the charge in a single bunch Q into n bunches of charge Q/n while maintaining the same net wakefield. It is much easier to produce a low emittance, short pulse electron bunch from a photoinjector at low charge than at high charge. Although the bunch train technique works to some degree for both structures, it will be of greater benefit to the harmonic device since the wakefield remains coherent for a longer distance. For the harmonic structure [Fig. 2(a)], we see that the second bunch should be placed in the decelerating

bucket near 46 cm, one net wavelength away from the first bunch. In this way, the excited wakefields from the different bunches (charge Q/n) will reinforce each other so that total wakefield, from n bunches, will approach that from a single drive bunch of charge Q. Close inspection of Fig. 2(a) shows that the peak accelerating field at 23 cm is greater than the peak field at 69 cm since the structure is not perfectly harmonic and some decoherence is obtained. Thus the wakefield excited by the bunch train will always be slightly less than that of the single charge. To understand why the bunch train technique is less beneficial in the single-mode structure we need to examine Fig. 2(b). In the single-mode structure, due to the highly nonharmonic wakefield excited, it is not clear where the second bunch should be positioned. The only choice is to place the second bunch one fundamental wavelength (for TM_{01} at 7.8 GHz, $\lambda = 3.8$ cm) behind the first bunch to reinforce the fundamental. But this means that the higher order longitudinal modes excited by the drive beam are parasitic and the energy is wasted, thus making the bunch train scheme less attractive for the single-mode case.

The parasitic HEM_{mn} modes driven by beam misalignments will not in general have the same frequency distribution as the TM_{mn} longitudinal modes [3,4]. Therefore, these HEM_{mn} modes will not in general be equispaced in frequency nor at multiples of the net longitudinal frequency and hence will not cohere at the location of a trailing accelerated bunch. If one can design a harmonic structure in which the longitudinal net wavelength and the transverse net wavelength are different, then the trailing bunches in the train would see no transverse wakefield if positioned in one of the long regions of nearly zero field. On the other hand, in the single-mode structure, where no regions of nearly zero fields exist, one can never expect better than a partial cancellation as has been thoroughly studied in [3,4]. Clearly, a detailed study of the transverse wakes in the harmonic structure is needed to study this question.

Using existing multipulse capabilities of the Argonne Wakefield Accelerator (AWA) facility [5], we have designed and constructed an experiment to demonstrate the synthesis of a predetermined wakefield pattern by multiple modes in a harmonic wakefield device. A train of four electron bunches, separated by one wavelength, was passed through a dielectric-loaded, approximately harmonic structure. The change in energy of the bunches in the train was measured and found to agree well with the design calculations and material assumptions for the structure used.

II. MULTIPULSE, HARMONIC DEVICES

In what follows, linear superposition holds so that the Green functions derived by Rosing and Gai [3] can be used to compute the wakefields for a bunch train. It is necessary to carry more terms in the calculation since a large number of the higher order modes are excited in the harmonic structure compared to a structure in which only a single mode is used for acceleration.

A. Wakefield due to a bunch train

It is trivial to extend the solution of Eq. (1) due to [3] for a single drive bunch to a "bunch train" of M bunches separated by a distance λ by writing the charge distribution as

$$f(z) = \sum_{m=1}^{M} f_m(z - m\lambda)\,. \tag{2}$$

The total wakefield $W_z(z)$ excited by the bunch train at any point z (which may be inside a bunch) is obtained by substituting the bunch train distribution of Eq. (2) into Eq. (1),

$$W_z(z) = \int_{-\infty}^{z} dz' \sum_{m=1}^{M} f_m(z' - m\lambda) \times \left\{ \sum_{n=1}^{\infty} G_n \cos[k_n(z - z')] \right\}, \tag{3}$$

where all variables are defined as in Eq. (1).

B. Comparison of harmonic structure and single-mode structure in the frequency domain

The difference between the spatial distributions of the harmonic and single-mode devices illustrated in the Introduction is best understood from frequency domain analysis. Using the same two structures that we used in the Introduction, the frequency spacing and the amplitude spectrum of the TM_{0n} modes are examined.

The harmonic nature of a mode spectrum is most easily seen by plotting the frequency difference between adjacent modes ($df_n = f_{n+1} - f_n$) vs the frequency of the nth mode (f_n). For a perfectly harmonic device we would have df_n equal to a constant. An examination of Fig. 3(a) reveals that the variation of the frequency difference [$\Delta(df) \sim 2$ GHz] varies by 12.2% over the single-mode spectrum, while Fig. 3(b) shows this variation [$\Delta(df) \sim 0.88$ GHz] to be only 6.3% over the multimode spectrum. Thus the multimode structure is seen to have a smaller variation, but not to be perfectly harmonic. In addition to the smaller variation in the multimode device, note that approximately 50 modes contribute to the wake in the frequency band under consideration for the multimode structure while only a few are driven in the single-mode case.

The amplitude spectrum can be calculated by multiplying the Green function amplitude G_n for each mode by the corresponding frequency domain Gaussian form factor value [the $f(z)$ of Eq. (1)] and plotting this vs mode frequency, $f_n = 2\pi/k_n$. Letting $\sigma_z = 2$ mm, we now plot the amplitude of the nth mode versus the frequency

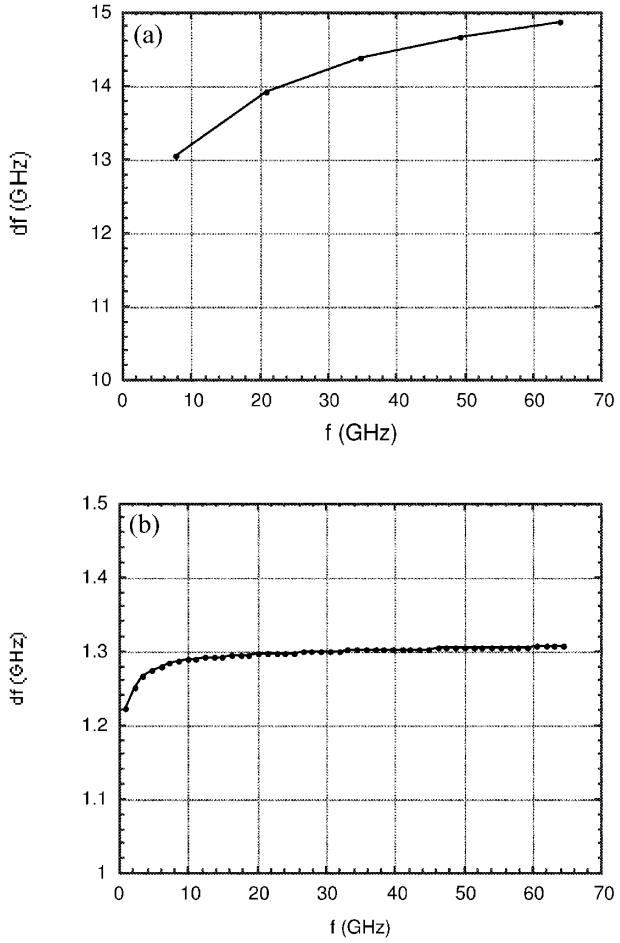

FIG. 3. (a) Frequency difference ($df = f_{n+1} - f_n$) vs frequency (f_n) for the single-mode structure. Note that df varies from ~13 GHz for $n = 1$ to ~15 GHz for $n = 5$. (b) Frequency difference ($df = f_{n+1} - f_n$) vs frequency (f_n) for the multimode structure. Note that df varies from ~1.2 GHz for $n = 1$ to 1.3 GHz for $n = 50$.

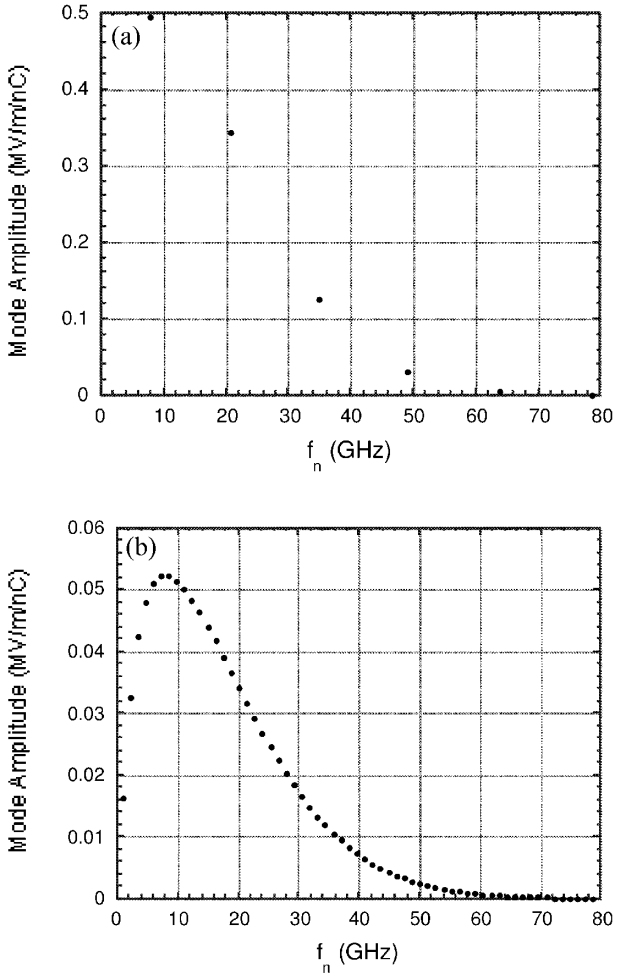

FIG. 4. (a) Amplitude spectrum for the single-mode structure. The TM_{01} mode ($f_1 = 7.8$ GHz) is the dominant mode excited. (b) Amplitude spectrum for the multimode structure. The TM_{07} mode ($f_7 = 8.5$ GHz) is the dominant mode excited, but many other modes are strongly excited as well.

of the nth mode for both the single-mode and the multimode devices described above. For the single-mode case [Fig. 4(a)], we see that the first mode (TM_{01}) is dominant. This is in stark contrast with the multimode amplitude spectrum of Fig. 4(b) where approximately 50 modes contribute appreciably and the largest amplitude mode is the 7th mode, not the fundamental. From Fig. 4(b) we see that the band of frequencies around the 7th mode contribute more strongly to the wake than those frequencies further away. This means that the band of frequencies contributing to the net waveform is more nearly harmonic than Fig. 3(b) would indicate. Quantifying this means that the frequency differences between these excited modes is nearly constant [$\Delta(df)/f < 3\%$] in the multimode structure. In contrast, only the first three modes are appreciably excited in the single-mode device, and its frequencies are not harmonically distributed.

In summary, the frequency difference between these excited modes is approximately constant for the multimode device, but not for the single-mode device. It is this feature that gives rise to the highly peaked spatial distribution of the multimode wakefield as seen in Fig. 2(a) compared to the cosinelike distribution of the single-mode structure in Fig. 2(b). This localization of the accelerating fields at delays of a whole number of wavelengths suggests that a multimode structure might have superior breakdown properties over a single-mode device where the fields are nonzero over a significant portion of a wavelength.

C. Multimode structure design for the AWA experiment

The choice of inner radius a and length L of the tube are constrained by the transverse emittance of the AWA drive linac and the desirability of maximizing the accelerating gradient in the structure. Since the AWA can provide a train of electron bunches with energy 15 MeV and emittance 20 mm mrad, an inner radius of 0.5 cm and tube

length of 60 cm were found to be capable of transmitting about 5 nC. The choice of dielectric constant was based on availability and was chosen to be $\varepsilon = 38.1$. The dielectric material [6] is a $CaTiO_3$-$LaAlO_3$ ceramic with a perovskite structure. With a and ε thus fixed, the outer radius b was adjusted so that the computed wakefield best approximated the shape expected for a harmonic structure with the interval between successive maxima equal to the distance between bunches (λ_{rf} in Fig. 1). For the multiple beam experiment at AWA, the drive bunch spacing is 23.05 cm since the linac λ_{rf} is 23.05 cm at 1.3 GHz; the outer radius b was computed to be 1.44 cm.

III. EXPERIMENTAL SETUP

The AWA drive linac is configured to provide a collinear bunch train of four bunches, each with charge $Q = 5$ nC, bunch length $\sigma_z = 4.5$ mm, and energy spread $(\Delta E/E)_{\mathrm{FWHM}} = 0.3\%$, separated by one linac rf wavelength λ_{rf}. To generate this electron bunch train, a laser bunch train is injected into the AWA drive photoinjector [5]. This laser bunch train is made by optically splitting a single laser pulse into four separate pulses with the combination of mirrors (M) and beam splitters (S) as shown in Fig. 5. The distance between bunches is varied via the optical delay lines, L1 and L2, which are adjusted by moving mirrors mounted on translation stages. Initially, the distance between bunches is coarsely set with a streak camera using the 10 ns sweep rate, providing a timing resolution of $\sim$10 ps between bunches. Final bunch spacing was done during the experiment by adjusting interbunch delays to maximize the energy loss of the trailing bunches after they emerged from the multimode structure.

Each bunch is spaced so that the individual wakes left by each bunch adds constructively to the wake of the preceding bunch. For the multimode experiment, simulation results show that the spacing between bunches must be accurate to a tolerance of σ_z for appreciable constructive interference to be obtained. Because the four drive beams must be spaced to within one σ_z to achieve significant acceleration, a high demand is placed on the AWA's energy measurement system. The energy measurement system must have a resolution of 0.5% or better and be insensitive to position jitter since bunches within the train may not follow the exact same path through the structure. To this end, a new imaging spectrometer was designed and built (Fig. 6) to provide improved momentum resolution over a wider range while reducing the sensitivity to beam jitter.

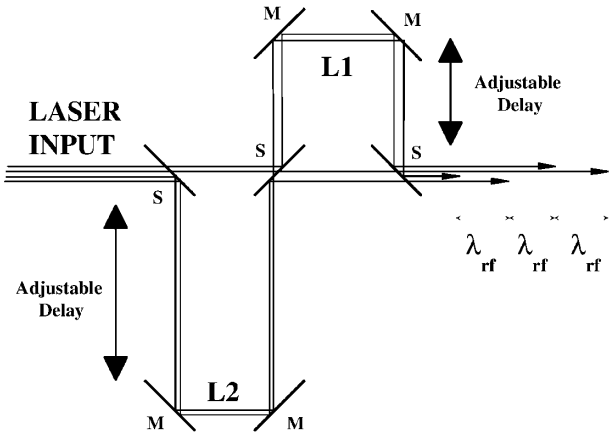

FIG. 5. Laser beam splitter optics. Three 50/50 beam splitters (S) in combination with four mirrors (M) are used to produce four laser pulses of variable separation. For this experiment, legs L1 and L2 are adjusted until the four pulses are separated by one wavelength of the rf (λ_{rf}) driving the photoinjector (lines separated for clarity.)

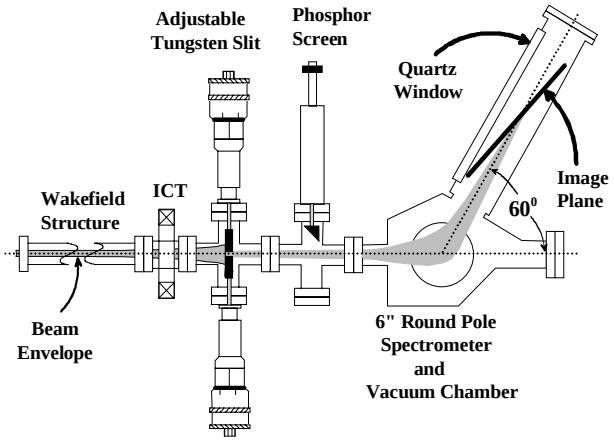

FIG. 6. Energy measurement system. The decelerated drive bunch train passes through a tungsten slit of adjustable width, which is imaged through a 60° dipole (diameter = 6″) onto a phosphor screen located at the image plane. The phosphor screen is viewed with an intensified camera through the quartz window.

To maximize transmission through the wakefield structure (Fig. 6), the upstream optics (not shown) are adjusted until a beam waist is centered in the structure. This is accomplished by maximizing the current passing through with integrating current transformers positioned at the beginning and end of the 60 cm long structure. Since there is no energy variation with transverse position in the beam emerging from the structure, we sample a small fraction of the beam with a tungsten slit located at the object point of the imaging spectrometer. The charge from the slit is imaged onto the phosphor screen at the image plane. Setting the tungsten slit opening to 300 μm, the resolution of the spectrometer is calculated to be 0.2%

IV. EXPERIMENTAL RESULTS

Using Eq. (3) (the expression for the wakefield excited by a bunch train), the computed wakefield as a function of z (the distance behind the first bunch) for our specific experimental parameters is plotted in Fig. 7. The parameters used to create the plot were a charge of 4.8 nC, rms bunch length of 4.5 mm, a FWHM energy spread of 0.3%, and an

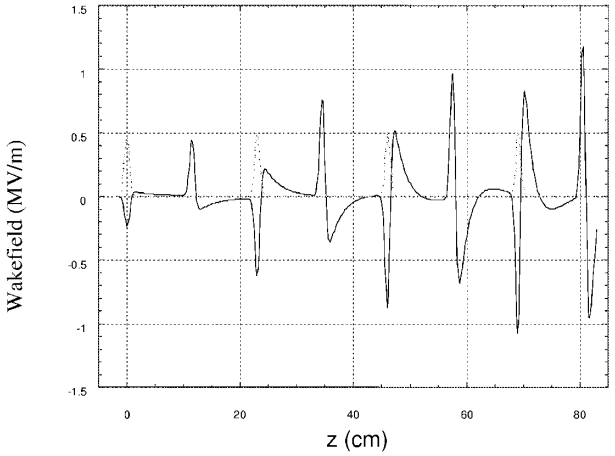

FIG. 7. The wake excited (solid line) by four monochromatic drive beams (charge = 4.8 nC each and bunch length = 4.5 mm) spaced one wavelength (23.05 cm) apart. The beam distribution is shown as the dashed line and is moving right to left.

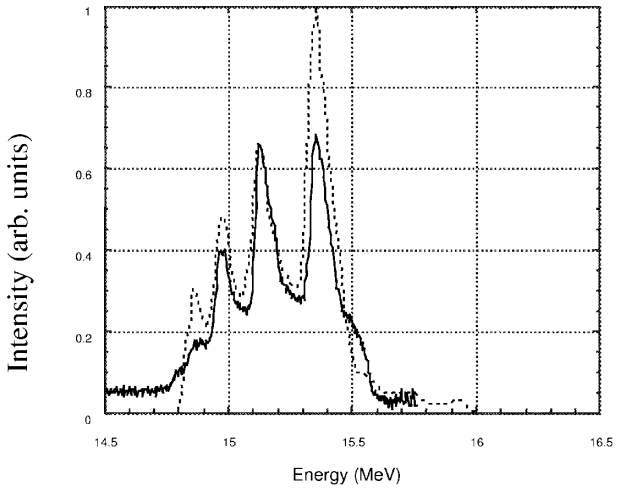

FIG. 8. Energy spectrum of the 4 × 4.8 nC bunch train. The solid line is the measured energy spectrum and the dotted line is the analytic fit.

initial energy of 15.46 MeV. From Fig. 7 one can see that peak accelerating wakefield is only about 1.2 MeV/m.

Using the computed wakefields (Fig. 7) one may easily extract the monochromatic energy spectrum generated by the four drive beams. Projecting the wake experienced by each particle within the bunch onto the energy axis and scaling by the appropriate value of L gives the monochromatic energy spectrum. The total energy spectrum is then computed by taking the convolution of the monochromatic energy spectrum over the energy distribution of the drive bunch, which is measured to be approximately Gaussian in shape.

The energy spectrum of the decelerated bunch train was measured at the image plane (Fig. 6) and acquired with a frame grabber for off-line analysis. For tube length $L = 59.87$ cm and the parameters given earlier in this section, we plot the measured energy spectrum (Fig. 8, solid line) and compare it to the computed energy spectrum (Fig. 8, dotted line). For the purposes of this experiment, the figure of merit is the location of the energy peaks in Fig. 8. The overall normalization of the individual energy peaks (here, intensity is proportional to the charge) is not related to the magnitude of the measured wakefield for a simple reason. Namely, the intensity variation at image plane (Fig. 6) is due to the fluctuations in transverse position of the individual bunches striking the 300 μm wide tungsten slit, thus causing the amount of charge transported to the image plane to fluctuate. These same transverse fluctuations do not affect coupling to the TM_{0n} modes. The energy peaks (in MeV) from the data are located at 15.35, 15.12, 14.98, and 14.88, while the fit peaks are located at 15.35, 15.12, 14.98, and 14.86. As is readily seen from this data, the agreement between theory and experiment is excellent. The data plotted in Fig. 8 is for a single shot. The relative energy separation between the bunches was very stable during the experiment ($<$10 keV) although the entire energy spectrum did shift ($\sim$200 keV) due to the energy fluctuation of the incoming bunch train due to the rf stability of the AWA facility.

To ensure that the measured energy spectrum was indeed due to wakefields and not the initial energy spectrum of the drive beams, the charge per pulse was reduced to $<$1 nC each without changing the bunch separation. Since the wakefield excitation amplitude is proportional to the total charge we expect the total width of the energy spectrum to be narrower in this case than in the high charge case. The projected energy spectrum of the low charge case is shown in Fig. 9. The narrow spread of the energy spectrum in Fig. 9 confirms that we are indeed seeing the effects of the multimode wakefield deceleration in the data of Fig. 7.

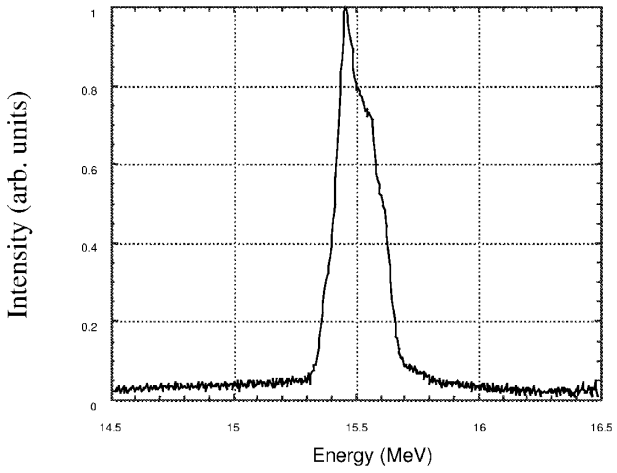

FIG. 9. Energy spectrum of low charge pulse train (4 × $\sim$0.5 nC) with an average energy of $E_0 = 15.46$ MeV. Total energy spread is observed to be much less than in the high charge case.

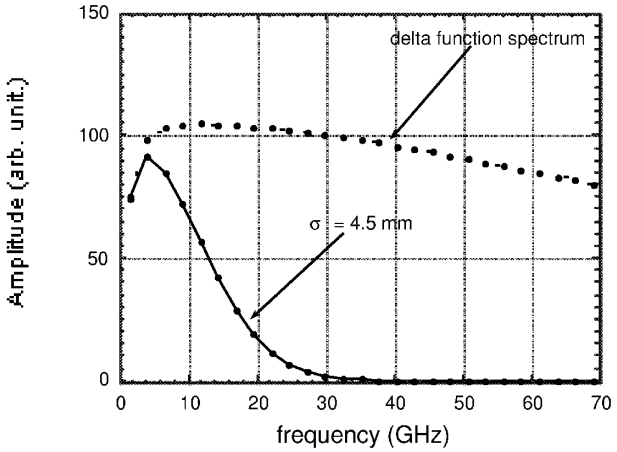

FIG. 10. Amplitude spectrum excited by a Gaussian beam with $1\sigma = 4.5$ mm (solid line) compared with the delta function amplitude spectrum (dashed line).

Because of the long bunch length used in this experiment we were able to infer the frequency dependence of the dielectric up to only ~30 GHz (approximately $1/2\sigma$) as seen from Fig. 10. In this figure we compare the amplitude spectrum excited by the beam of this experiment $\sigma_z = 4.5$ mm with that excited by a delta function beam. From this we find that the frequency dependence of the permittivity and loss tangent of the dielectric material used in this experiment is nearly constant up to approximately 30 GHz.

V. CONCLUSION

We have experimentally demonstrated the concept of multipulse driven wakefields in a harmonic dielectric structure. We have found that frequency independent dielectric materials are currently available which allow one to synthesize the wakefields needed for the multimode, harmonic accelerator. In addition, we found that the wakefield can be reinforced by a pulse train. The data agrees very well with our design calculations. Because of the fact that we used a dielectric tube with a relatively large inner radius, the observed gradient is low (1.2 MV/m), but the essential features of multimode wakefield synthesis have been validated. Investigation of high field effects such as structure breakdown and instabilities are not currently possible; planned facility upgrades will permit the latter measurements to be done. The new AWA photoinjector (under construction), with $Q = 5$ nC and $\sigma_z = 1$ mm, will permit the use of a dielectric structure to have inner radius of 2 mm and outer radius of 11.5 mm to achieve a 145 MV/m accelerating gradient.

ACKNOWLEDGMENTS

We appreciate the interesting ideas put forth by Dr. T-B. Zhang, Professor J. L . Hirshfield, and Professor T. C. Marshall and the useful discussions with Professor J. Rosenzweig and Dr. J. Simpson. This work was supported by the U.S. Department of Energy, Division of High Energy Physics, under Contract No. W-31-109-ENG-38

[1] T-B. Zhang, J. L. Hirshfield, T. C. Marshall, and B. Hafizi, Phys. Rev. E **56**, 4647 (1997).
[2] W. Gai, P. Schoessow, B. Cole, R. Konecny, J. Norem, J. Rosenzweig, and J. Simpson, Phys. Rev. Lett. **61**, 2756 (1988).
[3] M. Rosing and W. Gai, Phys. Rev. D **42**, 1829 (1990).
[4] K. Ng, Phys. Rev. D **42**, 1819 (1990).
[5] M. E. Conde, W. Gai, R. Konecny, X. Li, J. G. Power, and P. Schoessow, Phys. Rev. ST Accel. Beams **1**, 041302 (1998).
[6] E. A. Nenasheva, Mater. Res. Soc. Symp. Proc. **269**, 607 (1992).